Materials Research. 2020; 23(2): e20200063
DOI: https://doi.org/10.1590/1980-5373-MR-2020-0063

Rheo-Die-Casting of Al-Si-Mg Alloy and Al-Si-Mg/ SiC_p Composites: Microstructure and Wear Behavior

Sokkalingam Padmanaban[a]*, Ramanathan Subramanian[b], Jayapal Anburaj[b], Kuppusamy Thillairajan[b]

[a]PSG Polytechnic College, Department of Mechanical Engineering, Coimbatore, India.
[b]PSG College of Technology, Department of Metallurgical Engineering, Coimbatore, India.

Received: February 14, 2020; Revised: April 3, 2020; Accepted: April 14, 2020

In this paper, Rheo-Die Cast (RDC) Al-Si alloy with 7.5 wt % Si and 0.3 wt %Mg and Metal Matrix Composites (MMC's) of RDC Al-Si composites with 5 to 20 vol. % of SiC_p were produced by an in-house fabricated RDC machine. Microstructure and wear behavior of both RDC alloy and composites were investigated. Results indicated that the RDC samples have significantly refined microstructure with fine and uniform non-dendritic grains resulting increased hardness and enhanced wear resistance. Wear resistance is three times higher for sample with 20% SiC_p than those without SiC_p additions. Surfaces of wear test samples were investigated by SEM to study the effect of both grain structure and SiC_p particulates on the wear mechanism. It was also observed that reinforced RDC samples showed improved hardness and wear resistance due to the presence of SiC_p in the matrix of non-dendritic grains, obtained without modification treatment.

Keywords*: Aluminum alloy, composites, semisolid processing, microstructure, mechanical properties.*

1. Introduction

Aluminum-silicon alloy castings with a wide range of Si content have been extensively used in aerospace and automotive industry for the last two decades due to their high strength, low density, good castability, good corrosion resistance and weldability[1,2]. However, the applications of both gravity die-casting and high pressure die-casting aluminum alloys in high quality and integrity of components in automotive and aerospace sectors have been restricted due to their poor quality resulting from harmful gas entrapment in the solidified metal as well as the presence of large amounts of micro-porosity[3,4]. In recent years, rheological forming of semisolid metal such as Rheo-casting, Thixo-casting and Stir-casting of aluminum alloys have received wide attention in producing aluminum alloy castings with enhanced mechanical properties compared to conventional die casting processes[5-7]. In particular, the Rheo-Die-Casting (RDC) process is of significance in producing complex shape industrial components having high quality, high integrity and improved performance[6-8].

With advent of RDC process, undesirable dendritic microstructure (tree-like grains) of die casting Al-Si-alloys can be replaced with non-dendritic (fibrous grains) microstructure, which gives rise to an unusual improvement in strength along with improved ductility of the Al-Si alloy castings[9,10]. Many researchers have demonstrated the effect of processing parameters on the microstructure of rheo-die cast Al-Si-Mg alloys[11-14]. Paes and Zoqui[8] studied the microstructure of Al-Si-Mg alloys in the semisolid condition and reported high solid fractions in semisolid condition in Al-Si-Mg alloys with 4wt % to 7 wt % Si and 0.5wt % and 1.0 wt% Mg respectively. They also proposed a Rheo-cast Quality Index (RQI) for the Al-Si-Mg alloys to examine the thixo-formability of the modified aluminum alloys. A high RQI value indicated a good thixo-formability of the modified alloys. This value is related to low silicon content in the aluminium alloy. However, low silicon content leads to high viscosity values and is usually not suitable for good thixotropic behavior required for semisolid processing[15]. Birol[16] studied the microstructure of semi-solid processed A356 die-casting alloy and found that the solid fraction linearly increased in semi-solid temperature range.

Tzamtzis et al.[17] have reported that aluminium metal matrix composites have also emerged as advanced materials for several engineering applications, in particular automotive and aerospace sectors due to their excellent combination of properties like high strength, high stiffness, electrical and thermal conductivities, low coefficient of thermal expansion along with better wear and seizure resistance[18,19]. These metal matrix composites have found to be an effective functional materials, especially in break drum, cylinder liners and cylinder blocks[20-22]. Esmaily et al.[20] found that the wear volume of metal matrix composites increased with both increasing sliding distance and applied load. They also reported that presence of SiC_p was found to be effective in increasing wear resistance of the composites. Studies on mechanical properties and wear behavior of RDC Al-Si alloys with SiC_p reinforcement are very limited. Main aim of the present work is to produce the RDC Al-Si-Mg alloy with SiC_p reinforcement using an in-house fabricated Rheo-Die-Casting (RDC) process and to comparatively study the effect of non-dendritic grains on the mechanical properties of RDC alloys those of with high pressure die-casting alloy. In addition, the effect of SiC_p on the grain size, hardness and wear resistance of the Al-Si-Mg composites with different percentages of SiC_p was also investigated.

*e-mail: padmanaban09ind@gmail.com.

2. Materials and Methods

2.1 Materials

In the present work, die cast A356 aluminium master alloy ingot was used as the master alloy whose chemical composition analysis by optical emission spectrometer is given in Table 1.

This alloy was chosen in the present study, since it facilitates easy ejection and helps die release in high pressure die casting process[20]. Moreover, this alloy is also designed for RDC process since it has relatively long freezing temperature range, i.e. the liquidus and the solidus temperatures are 615°C and 570°C respectively. This aids in more slurry formation in the liquid during RDC process. In addition, the RDC alloys with different percentages of SiC_p with average size of 5-10 µm to produces MMC's. Figure 1 shows the RDC sample of Al-7.5 wt %Si-0.3 wt %Mg alloy as well as SiC_p reinforced RDC sample produced by the in-house designed and fabricated RDC equipment.

2.2 Preparation of RDC alloy and SiC_p reinforced RDC composites

RDC alloy of Al- 7.5 wt % Si- 0.3 wt % Mg and RDC composites of Al- 7.5 wt % Si-0.3 wt % Mg alloy with 5 -20 vol. % SiC_p, in increment of 5 vol. %, were produced. Initially, A356 alloy ingots were melted in an Inconel metal crucible using a resistance type melting furnace at a temperature of 750°C, followed by degassing with degassing flux tablets in order to remove the dissolved gases in the liquid metal. Subsequently, the liquid metal was transferred into slurry maker to achieve semisolid slurry which was then directly injected into a die cavity for forming desired sample shape with help of plunger using an external pressure of 100 MPa. In case of MMCs, the carefully weighed amounts of SiC_p were preheated at 600°C for 2 hours in an electric resistance heat treatment furnace to remove the surface impurities and assist in adsorption of gasses. These SiC_p particulates were slowly added to the liquid metal with continuous stirring for 1minute at approximately 250 rpm.

Figure 1. Rheo-Die- Cast (RDC) Al-Si-Mg alloy and composite samples

The composite liquid metal was then poured into the slurry maker to get semisolid composites. Then the semisolid slurry with high viscosity composite was injected into die cavity for forming the samples (Figure 1) with dimensions of 75 mm length and 25 mm diameter.

2.3 Microstructural investigations of RDC samples

Microstructural characterization was carried out for both RDC alloy and reinforced RDC composites using a Carl Zeiss optical microscope equipped with image analyser facility and Scanning Electron Microscopy (Model: JEOL JSM6360) was also carried out. Samples for optical microscopy were prepared by standard metallographic techniques and etched for 40-50 seconds in Keller's reagent (190 mL distilled water, 5 mL HCL, 3 mL HNO_3, 2 mL HF).Phases present and their distributions were studied using optical microscope. The volume fractions and size of primary silicon particles present in the matrix for all the RDC samples were quantified using image analyzer. Further, the grain size and volume of SiC_p present in the microstructures of the metal matrix samples were also measured by image analyzer.

2.4 Evaluation of hardness and wear behavior of RDC samples

Hardness tests were carried out on both RDC alloy and RDC composites using a Mitutyo micro-hardness tester under a load of 100g for 15 seconds. Average of five readings measured at different locations across the cross section of the sample was taken as hardness value. Wear samples of 10 mm width, 10 mm thickness and 25 mm length were prepared from both RDC alloy sample and metal matrix RDC samples for wear tests (confirming to ASTM G99 standard). The wear behavior of these samples was investigated using a pin-on- disc type wear testing machine under dry sliding conditions. Samples were tested at rotational speed of 1000 rpm and an applied load of 50N. The diameter of the wear track was fixed at 100 mm and the test time was varied between 1 minute and 5 minutes.

The wear test samples (i.e., pins) were weighed accurately prior to and after the test using a high precision electronic balance. The volume (mm^3) and wear rate (mm^3/m) of the tested samples were calculated using the following formula as shown in Equation 1 and Equation 2[23]:

$$wear\ volume,\ mm^3 = (mass\ loss,\ g)\ x\ 1000\ /\ \left(density,\ g/cm^3\right) \quad (1)$$

$$wear\ rate,\ mm^3/m = \Delta m\ /\ \rho L \quad (2)$$

where Δm is the mass loss (g); ρ is the density (g/cm^3) ; L is the sliding distance (km).

Worn-out surfaces of samples were examined by SEM (model: JEOL JSM6360) to study the wear behavior of both RDC alloy samples as well as the reinforced composite RDC samples.

Table 1. Chemical composition (in wt %) of A356 alloy ingot.

Elements	Si	Mg	Cu	Fe	Mn	Ti	Zn	Ni	Al
Wt %	7.43	0.32	0.01	0.21	0.021	0.026	0.04	0.037	Bal.

3. Results and Discussion

3.1 Microstructural examination

Influence of semisolid metal on the microstructure of RDC Al-Si-Mg alloy was investigated and compared with High Pressure Die-Cast (HPDC) sample. Figures 2a and 2b shows the microstructures of the alloy produced by HPDC technique and RDC techniques respectively. The HPDC alloy shows a typical structure consisting of primary eutectic α-Al dendrite grains with needle-like or acicular eutectic Si particles (Figure 2a). As evident from the microstructure of the HPDC alloy, a typical tree-like structure having unmodified Si particles was observed and it is caused by a relatively high cooling rate during solidification in the metallic mould. The presence of unmodified Si particles (needle-like Si particles) or acicular Si particles in the Al-Si alloy is generally considered to be undesirable, since they act as potential sites for stress concentration leading to catastrophic failure under sudden loading or provide an easy path for propagation of cracks during brittle failure[24].

In the RDC alloy, the eutectic Si particles were found to be very fine and uniformly distributed in the matrix as compared to the HPDC Al-Si alloy as seen in Figures 2a and 2b. On the other hand, RDC processed sample revealed a microstructure consisting of uniform and fine non-dendritic α_{Al} eutectic grains with finely dispersed eutectic Si particles (Figure 2b). This modification in the microstructure of RDC alloy confirms that the RDC equipment is capable of producing sufficient quantities of slurry particles, which aids in converting the microstructure from dendrite grains to non-dendritic or fibrous grains in Al-Si alloys. The formation of non-dendrite grains in RDC alloys depends on the several factors such as (i) slurry volume (ii) shear rate (iii) viscosity of the semisolid metal(iv) freezing temperature of alloy and (v) cooling rate as reported by Sato[12].

Several researchers[6,11] have stated increase in the viscosity of the slurries leads to agglomeration of globular particles. It has been reported that the semisolid slurries controlled by above rheological parameters are very critical in RDC process. Wannasin et al.[5]studied the effect of solid fraction in the RDC alloys and reported that the apparent viscosity of the sheared semisolid slurries increases with increase in volume fraction solid and cooling rate, while it decreased with an increase in shear rate. They also concluded that the RDC alloy showed higher amounts of dendritic grains in the matrix at higher cooling rates. Further, microstructural analysis indicated the absence of micro porosity and gas entrapment in the RDC sample. However, a very few particles of Fe bearing intermetallic compounds were observed in the matrix of RDC alloy (Figure 3). The morphology of this compound is totally different from the conventional metal mould process, because the intermetallic compound in the RDC alloy shows highly dispersed spherical particles compared to HPDC alloy, where the Fe compounds were present in the form of stringer morphology. Commercial Al-Si ingots usually contain some Fe impurities in form of intermetallic compounds, which are detrimental to mechanical properties, in particular on elongation in Al-Si alloy castings processed by HPDC[16]. On the other hand, aluminum master alloy containing high iron content is added deliberately sometimes to Al-Si alloy in order to increase resistance to die erosion in HPDC Al-Si alloy castings[19]. However, the presence of fine and spherical Fe-bearing intermetallic compounds is also less detrimental to mechanical properties of RDC samples, in particular elongation and toughness. These finely distributed intermetallic particles play an important role to suppress the growth of the fibrous Al eutectic Al grains as reported by Sato[12].

A comparison of the density of both HPDC alloy and RDC alloy showed that the density of RDC sample is close to the theoretical density (2.61 g/cc) compared that of HPDC sample (2.42 g/cc) confirming the absence of porosity in the RDC sample. The ability of RDC machine in producing high quality semisolid alloy with better microstructure was also corroborated. Complete elimination of micro-porosities in RDC sample could be attributed due to the two reasons: (i) semisolid alloy is freezing at a relatively lower temperature, which helps in removing the dissolved gas readily and (ii) plastic deformation of semisolid metal in mushy condition prior to the commencement of freezing. In comparison, freezing

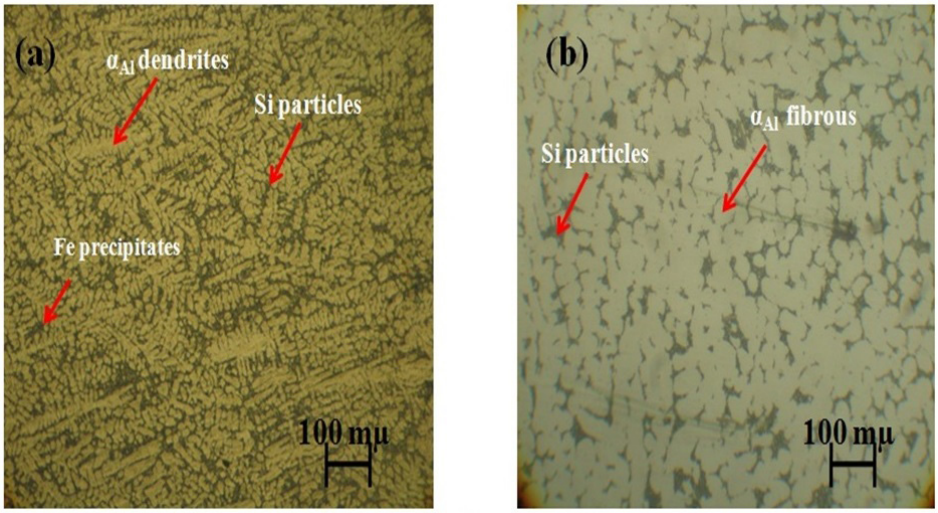

Figure 2. Optical micrograph of (a) HPDC Al-7.5wt % Si -0.3 wt % Mg alloy and (b) RDC Al-7.5 wt % Si -0.3 wt % Mg alloy

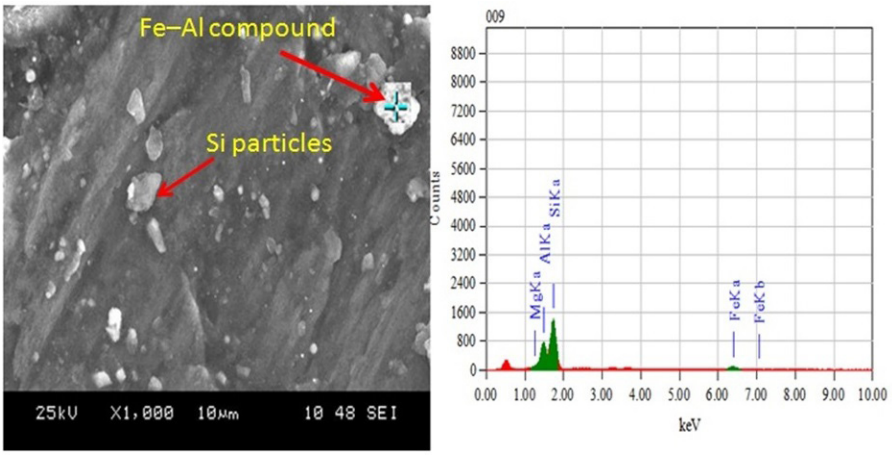

Figure 3. SEM with EDS result of the RDC alloy showing the Fe-rich compound in the matrix.

occurs at a higher temperature, leading to gas entrapment and porosity resulting reduction in density in the case of HPDC samples.

Another significant feature associated with RDC alloy is the formation of fibrous non-dendritic grains in the matrix (Figure 2b). Solidification of RDC alloy occurs in two stages: in the first stage, primary solidification begins where solid fractions are formed in excess of 50% sufficient enough to form a globular microstructure. Due to high shear rate caused by the slurry maker, nucleation rate is increased significantly, further promoting the spheroidal grain formation by reducing the thickness of thermal and solute diffusion boundaries layer at the solid /liquid interface during solidification[11,17]. The second stage differs from primary solidification and is characterized by high cooling rate with plastic deformation of the semisolid slurry. This results in a homogeneous temperature gradient as well as chemical composition gradient in the alloy. Past research work have concluded that the solidification proceeds by a process of nucleation and growth in the remaining liquid metal and possibly every nucleus is expected to become more stable and contribute equiaxed grains to final microstructure of the alloy[16,17]. The microstructure of present RDC alloy (Figure 2b) is in agreement with the above findings. Use of metallic die provides a very high cooling rate leading to enhanced nucleation rate in semisolid metal, Fan et al.[4] have reported a similar results of semi solid processed Al-Si alloys with different concentration of Si and Mg contents. Another consequence of high cooling rate is the non-equilibrium structure resulting in the formation of increased amounts of divorced eutectic Si phase along the grain boundaries in the matrix of α-Al. SEM micrograph confirms the formation of divorced spherical eutectic Si phase in the RDC alloy (Figure 4).

Figures 5a and 5b show SEM micrographs of HPDC alloy and RDC alloy respectively. The HPDC alloy typically consists of primary α-Al dendritic grains and non-uniform distribution of needle-like eutectic Si particles with needle-like morphology and an average plate thickness of 2µm to 4 mm and a length of 25-35µm (Figure 5a).

The SEM microstructure of RDC alloy (Figure 5b) shows non-dendritic α-Al aluminum grains and spherical shape Si

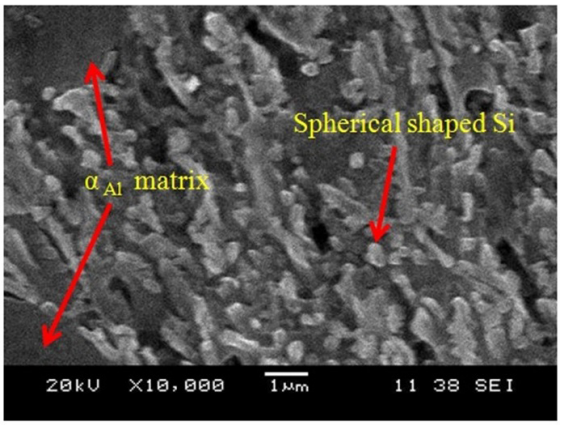

Figure 4. SEM micrograph showing the distribution of spheroidal eutectic Si phase in the RDC alloy.

particles segregated. In the RDC alloy, the Si particles are very fine and uniformly distributed throughout the sections. In contrast, the HPDC alloy showed both plate and needle-like Si particles, which promote brittleness[15]. This undesirable microstructure can be modified by the addition of modifying agent (either Na or Sr) during melting. However, in the RDC alloy modification of both size and shape fine and spherical particles without additions of modifying agents to the liquid metal. The size and shape of the RDC Al-Si alloy was evaluated using empirical equations[16].

$$D = \frac{\sum_{i=1}^{N} \sqrt{4Ai/\pi}}{N} \tag{3}$$

$$Fs = \frac{N}{\sum_{i=1}^{N} \frac{Pi^2}{4\pi Ai}} \tag{4}$$

where

D- the equivalent grain diameter (mm)

Fs- the average shape coefficient

A- the area (mm^2)

N- constant

P- the perimeter of the primary grains (mm).

Using Equations 3 and 4, the size and shape of the α-Al grains were estimated for the RDC alloy. The shape factor fractions for these two samples were also calculated and were found to be 0.3 and 0.95 respectively. The average grain size observed using image analyser (Figures 2a and 2b) for both HDPC and RDC alloys were approximately 33.0 µm and 22.0µm respectively. Subsequently, the average grain size using empirical equations calculated for HPDC alloy and RDC alloy was approximately 36.0 µm and 21.0 µm respectively. From these results, it is evident that the grains in the RDC sample are found to be significantly finer in size and spherical in shape compared to the HPDC alloy for the same composition. The average grain size of both HPDC and RDC samples (33.0 µm and 22.0 µm respectively) observed by image analyzer measurements is well supported by empirical equations.

RDC alloy based metal matrix composites were investigated to study the effect of SiC_p on the microstructure and mechanical properties and compared with HPDC alloys. Optical micrograph of metal matrix composite RDC samples for different percentage of SiC_p particles ranging from 5 vol. % to 20 vol. % at an increment of 5 vol. % are shown in Figure 6. It can be seen that the shape of non-dendritic grains in the matrix of metal matrix RDC samples does not change with increase of SiC_p (Figure 6). In addition, the optical micrograph of the metal matrix RDC samples confirms the uniform distribution of SiC_pparticles in the matrix, as seen from Figures 6a to 6d. This is due to

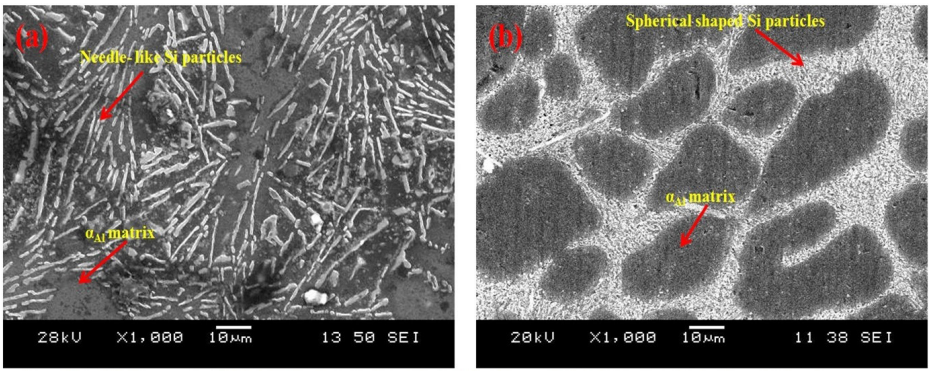

Figure 5. SEM micrographs of (a) HPDC Al-7.5 wt % Si- 0.3 wt % Mg alloy and (b) RDC Al-7.5 wt % Si- 0.3 wt % Mg alloy

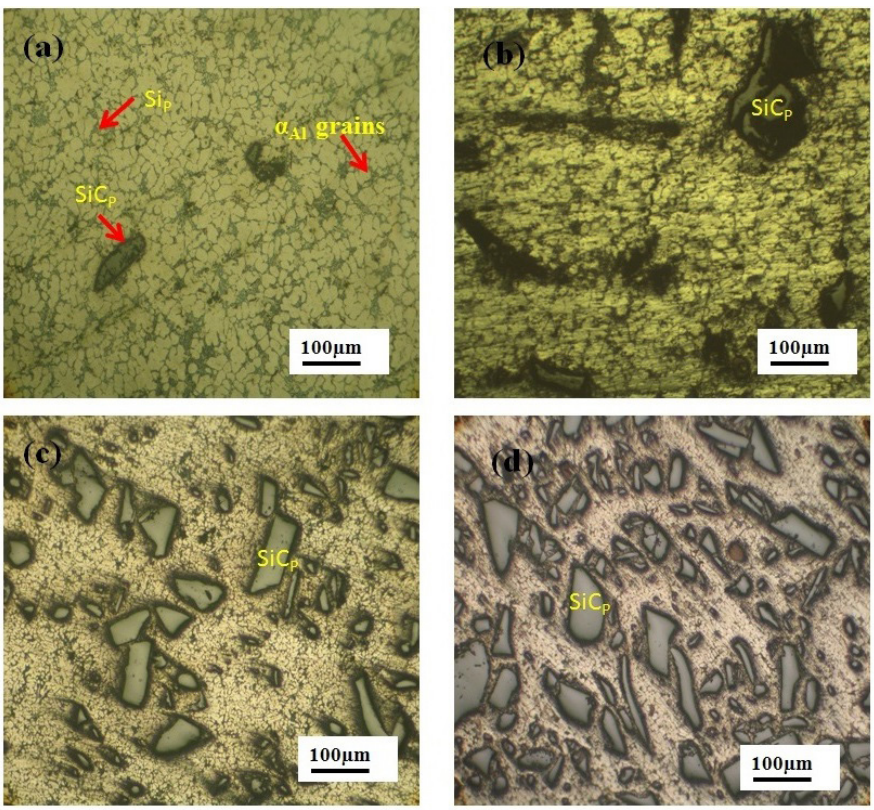

Figure 6. Optical micrographs of RDC Al-7.5wt %Si-0.3 wt % Mg reinforced with (a) 5 vol. % SiC_p, (b) 10 vol. % SiC_p, (c) 15 vol. % SiC_p and (d) 20 vol. % SiC_p.

the effect of spiral screw rod slurry maker, which provides the effective mixing of SiC_p within liquid metal through impellers, prior to the deformation of semisolid metal in RDC process. Further, the most of the SiC particles were found to have excellent bonding with the matrix.The size of eutectic α-Al non-dendritic grains was measured for all the RDC composite samples using the empirical Equation 3 (Table 2).

From Table 2, it can be observed that the size of α-Al non dendritic grains in RDC composites decreased from 22µm to 9 µm as the SiC_p content increased up to 20 vol. %. This reduction in grain size can be attributed to heterogeneous nucleation caused by SiC_p. The addition of SiC_p changes the liquid-solid interfacial energy sufficient enough to assist more nucleation, thereby reducing the amount of super cooling required to cause the nucleation[25]. Presence of non-dendritic fibrous microstructure in RDC alloy can also be attributed to the increasing amounts of external heterogeneous nucleation agents which give rise to formation of ultrafine grains with globular Si particles. This statement is in good agreement with the results of the RDC aluminium alloys reported by Tzamtzis et al.[17].

Figure 7 shows the SEM micrographs of metal matrix RDC samples with different percentage of SiC_p reinforcement. A uniform distribution of SiC_p particles throughout the cross section can be observed in all the samples. From Figure 7, angular morphology of SiC_p particles and absence of porosity can be clearly seen.

An important feature seen from Figure 7 is that the excellent bonding of SiC_p with the matrix compared to the conventional stir cast alloys. In RDC composites, the spiral screw rod slurry maker helps to distribute the SiC_p particles uniformly in the matrix. Enhanced mixing of SiC_p with liquid alloy is promoted by the high shear force induced by the spiral screw rod. According to Tzamtzis et al.[17] intensive shearing is required to form dispersed particles by applying a shear stress that will overcome the cohesive force of the cluster. The degree of mixing of SiC_p particles with liquid metal can be significantly influenced by various factors like (i) distance of the cluster particles from the stirrer, (ii) shear force applied to the impeller and (iii) the viscosity of the liquid medium[17,24].

3.2 Evaluation of hardness of RDC alloy and composites

Average hardness of both RDC sample and metal matrix RDC samples reinforced with different percentage of SiC_p is shown in Table 3. The hardness of RDC alloy is around 76 $HV_{0.1,}$ which is relatively lower when compared with HPDC alloy (84 $HV_{0.1}$) having needle like Si particles. This is due to both fibrous shape and uniform distribution of Si particles (modified Si phase). No abnormalities are observed in the matrix of the RDC alloys. In the case of metal matrix RDC samples, the maximum hardness of 144 $HV_{0.1}$ for sample with 20% SiC_p and the minimum hardness of 93 $HV_{0.1}$ for sample with 5 vol. % of SiC_p were evaluated. With addition of SiC_p reinforcement, the hardness of the RDC alloy by more than 2 times and this represents a significant improvement in wear resistance of the Al-Si alloy rather than increasing Si content alone. The observed increase in hardness can be attributed to both uniform distributions of SiC_p particles as well good bonding of SiCp with matrix due to better

Table 2. Average grains of α-Al grains as a function of % SiC_p in RDC composites.

Sample details	RDC composites with vol. % of SiC_p				
	0%	5%	10%	15%	20%
The average grain size (µm)	22 ± 2	20± 2	17± 2	12± 2	09± 2

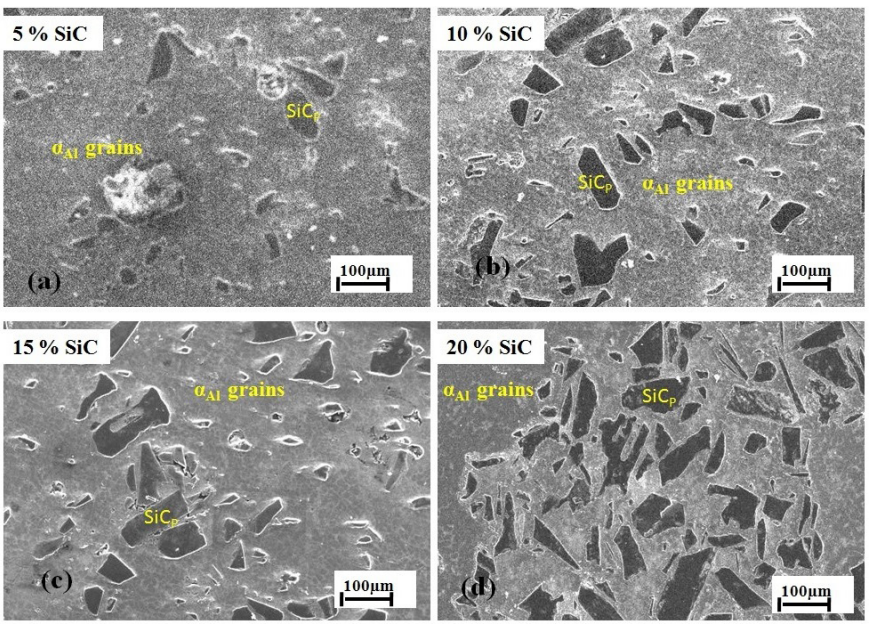

Figure 7. SEM micrographs of metal matrix RDC Al-7.5 wt %Si- 0.3 wt % Mg samples reinforced with (a) 5 vol. % SiC_p, (b) 10 vol. % SiC_p, (c) 15 vol. % SiC_p and (d) 20 vol. %SiC_p.

wetability. This result is in good agreement with results of several reported investigations[25]. As seen from Table 3, the fine grain size and improved distribution of SiCp particles during RDC process account for an increase in hardness of the metal matrix composite RDC samples.

Rao et al.[24]have reported that the hardness of the metal matrix Al alloy is strongly dependent on the amount and distribution of the SiC_p in the matrix. Increasing volume of SiC_p reinforcement in Al-Si alloy increases the dislocation density due to thermal expansion mismatch between the matrix and the reinforcement leading to an increase in high hardness of the matrix[20,25].Basavakumar et al.[26] have reported that the number of SiC_p particulate increases considerably in the matrix with decreasing the size of the reinforcement particulates and a consequent increasein the dislocation density of the matrix[27].

3.3 Wear behavior of RDC alloy and composites

Figures 8a and 8b shows the wear test results indicating the wear volume (mm^3) and wear rate (mm^3/m) of the HPDC alloy, RDC alloy and RDC composites at a constant pressure (0.85 N/mm^2) as a function of sliding distance. The wear volume of both HPDC and RDC samples increased markedly with an increase in the sliding distance. In contrast to HPDC alloy, RDC alloy shows a steady wear volume up to a sliding distance of 15 km, after which the wear volume increased significantly with further increase in sliding distance, similar to that of the HPDC alloy. For the same chemical composition of Al-7.5 wt %Si-0.3% Mg alloy, the wear volume of RDC alloy was observed to be 16.2 mm^3 at a sliding distance of 5 km compared to the HPDC alloy, which showed a relatively high wear volume of 24.6 mm^3, i.e. 50% more wear volume than RDC sample. This marked improvement in wear resistance can be attributed due to the presence of (i) fine grained eutectic α_{Al} structure with uniform distribution of globular Si particles and (ii) non-dendritic grains, which provide a cushioning effect in resisting the de-lamination of the matrix under compressive load during wear test.

RDC samples showed abnormal wear rate at higher sliding distance of 30 km. At sliding distances below 15 km, the increase in wear rate of the RDC sample was found to be very low and constant. However, at higher sliding distances, a higher wear rate with abnormal wear loss was observed. This higher wear rate can be attributed to the formation of oxide layer, which influenced the frictional force at the interface of pin and disc causing three body abrasions. In addition, at longer sliding distances, high frictional force generates more heat which in turns often the matrix leading to plouging of the matrix and producing more debris. Similar to wear volume, the wear rate of all the HPDC alloy, RDC alloy and RDC composites increases nearly linearly with an increase in sliding distance at a constant applied load (Figure 8b). Compared to RDC alloy, RDC composite samples exhibit much higher wear resistance with the wear rate of these samples being very low even at increasing sliding distance up to 30 km. At a sliding distance of 5 km, the wear rate of RDC composite sample with 20 vol. % SiC_p is nearly 3 times lower than that of the RDC sample without SiC_p additions.

The observed wear rate of RDC composite sample with 20 vol. % SiC_p at a sliding distance of 30kmcan be observed to be 6 times lower than those of the RDC alloy sample under the same condition (Figure 8b). In addition, all the metal matrix RDC samples show a steady and slow wear rate with increasing sliding distance irrespective of the percentage of SiC_p additions. The reduction in wear rate of the RDC composites with different percentage of SiC_p can be attributed to the increase in hardness caused by grain refinement as well as presence of SiC_p and increased dislocation density. In contrast to RDC alloy, RDC composite sample showed minimum wear under frictional loading.

The fabricated RDC machine not only results in minimum micro-porosity, but also leads to refinement of the microstructure from random dendritic grains to fine and uniform non-dendritic grains. Such a microstructure enhances both the wear resistance as well as mechanical properties. Generally spherical shaped particle results in higher resistance to sliding wear than that of the needle like

Table 3. Average hardness of RDC alloy and RDC composites

RDC Composites with vol. % of SiC_p	Average hardness ($HV_{0.1}$)	%of increase in hardness
0	76 ± 3	-
5	93± 3	20
10	118± 3	50
15	132± 3	79
20	144± 3	90

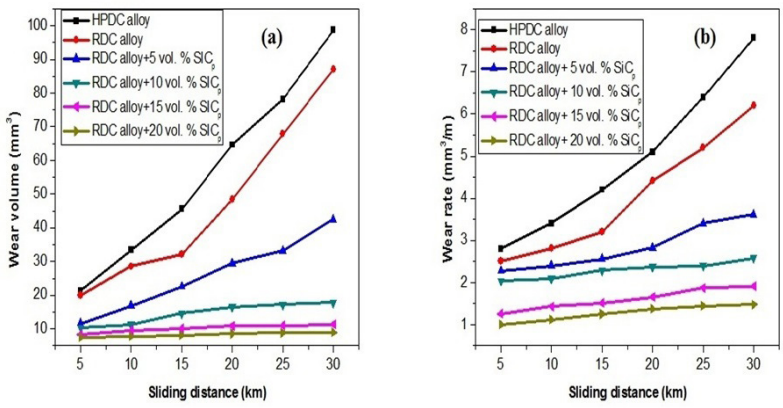

Figure 8. Wear results of the HPDC alloy, RDC alloy and RDC composites: (a) wear volume vs. sliding distance and (b) wear rate vs. sliding distance.

Si particles[28,29]. Elmadagli et al.[23] reported a decrease in the wear rates and volume with increasing sphericity of the Si particles. The presence of spherical shape grains reduces the tendency to fracture. As reported in the present work, a sphericity value of 0.9 was observed for Si phase in the RDC alloy compared to a sphericity value of 0.3 for the HPDC alloy. These results are in good agreement with reported literature[28]. It is also observed that the improvement in the wear resistance of the RDC alloys with modification of grain size and Si particle morphology by Rheo-casting process, correlates with the improvements in mechanical properties, in particular the hardness of RDC alloy as seen from Table 3.

Apart from the microstructural characteristics of RDC alloy, some literature studies demonstrated that the additions of SiC_p particles facilitate the compaction of the oxides favoring the formation of oxide layer during wear, which acts as a protective layer[30]. Thus in the case of composites, a oxidative mechanism is more predominant up to higher speeds and loads compared to materials without reinforcement of SiC_p particles[30].

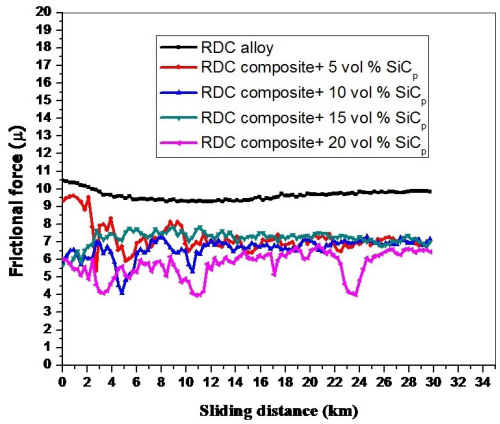

Figure 9. Frictional force on RDC alloy and RDC composites as function of sliding distance.

Figure 9 shows the resultant frictional force on the RDC alloy as well as RDC composites with different percentage of SiC_p particles as a function of sliding distance at a constant applied pressure of 0.85 N/mm^2. It is clearly seen that the RDC alloy shows much higher frictional force with increasing sliding distance. The average frictional force of RDC alloy was found to be about 10.5μ and remained nearly constant with increasing sliding from 0 to 30 km. This can be attributed to the presence of fine and spherical Si particles in non-dendritic grains.

Unlike RDC alloy, the RDC composites show more variations of frictional force with increasing sliding distance. In particular, the frictional force of the RDC samples decreases markedly as the percentage of SiC particles increases from 0 vol. % to 20 vol. %. Sample with 20 vol. % SiC_p particulates showed to have large variations in frictional coefficient i.e. the frictional coefficient of 20 vol. %SiC_p metal matrix sample varies from 6.6 μ to 3.0 μ with increasing sliding distance in comparison to sample with 15 vol. % SiC_p particulates. Thus it is clear that the frictional force is influenced by the percentage of SiC_p in the matrix of RDC composites. The relatively higher wear of the RDC alloy results from the high frictional force.

3.5 SEM investigation of worn-out surfaces of RDC alloy and composites

SEM micrographs (Figure 10) of the worn surfaces of the HPDC and RDC alloy tested for 5 km and 30 km of sliding distance respectively. At a sliding distance of 5 km, the worn surface of both HPDC alloy and RDC alloy showed continuous parallel and shallow grooves on the surface along the direction of contact. The surface also shows the initial stage of formation of micro-grooves, craters and scoring marks that are very small in size in the case of RDC alloy. As sliding distance

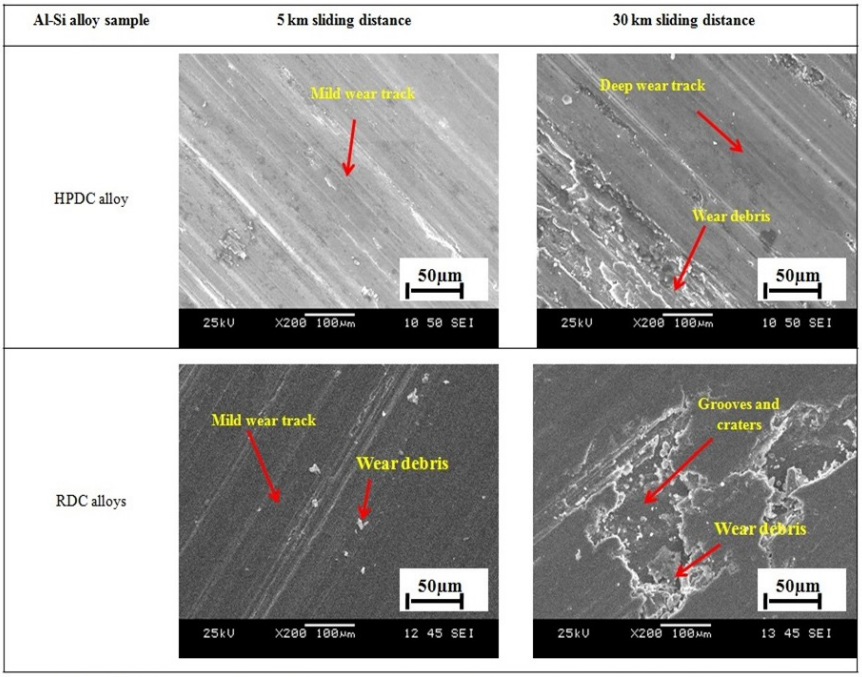

Figure 10.SEM micrographs of the worn surfaces of HPDC alloy and RDC alloy at 5 km and 30 km of sliding distance.

increases, typical wear features like micro-grooves, craters and abrasive scoring marks were observed for worn surface of the both samples. The micro-grooves occur initially in the direction of the deformation zone in the matrix. Since the friction coefficient is high at low sliding distance, this causes the metal surface to yield permanently forming micro-voids and craters along the direction of the deformation. These grooves and craters lead to subsequent delamination of the matrix under the influence of frictional force. The size of the grooves and crates are controlled by several factors, in particular the composition of the alloy and the sliding distance. As sliding distance increases, the depth of groove and craters in the matrix increased significantly. HPDC alloy shows (Figure 10) multiple grooves which are slightly larger in size compared to RDC alloy at 5km sliding distance. On the other hand, the worn-out surface of the samples at sliding distance of 30 km shows large grooves and craters much deeper than the samples tested at low sliding distance. The abrasive wear behavior of material is generally controlled by the mechanical and metallurgical characteristics of the alloy in addition to the wear test parameters like applied load, sliding distance and abrasive medium.

For HPDC alloy and RDC alloy, the reasons for formation of more debris during normal loading are low hardness of the matrix. This is in good agreement with the results of investigation done by Elmadagli et al.[23]. As seen from the optical microstructure (Figure 2b), RDC processing has led to the refinement of microstructure, in particular the grain size and shape of Si particles. This improved microstructure gives rise to an increase in hardness in case of RDC alloy and consequently a high wear resistance, as expected from the Archard's law[31].

Figure 11 shows the worn surface of the metal matrix RDC samples with different percentage of SiC_p additions at 5 km and 10 km sliding distance.

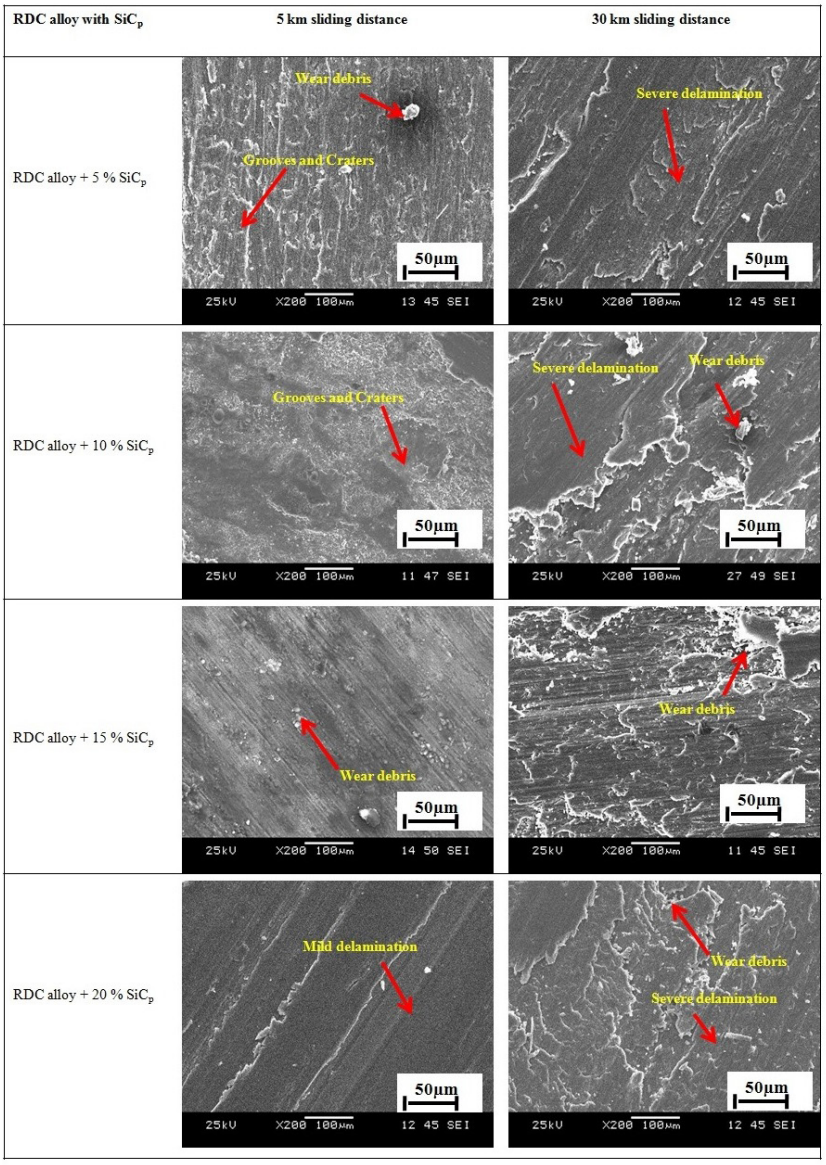

Figure 11. SEM micrographs of the worn surfaces of the RDC composites with different volume percentage of SiC_p.

The worn surfaces of the RDC composites also show abrasive grooves and craters similar to the RDC alloy. However the width and depth of the grooves and craters are limited due to the presence of hard SiC_p which provides better resistance to abrasion. However, the groves and craters in the deformed areas continue to grow its size with increase in sliding distance from 5km to 30 km. Removal of the metal surface under frictional load occurred through ploughing and micro-cutting. These mechanisms require penetration by hard abrasive particles which in turn are limited by the hardness of the alloy[31]. The weight loss of metal surface due to delamination can be directly related to the volume of debris produced. At higher sliding distances, the continuous action of lamination and delamination of deformed wear surface caused bulk removal of metal by deep grove formations. It is also important to note the decrease in the depth of grooves and craters in case of increasing additions of percentage of SiC_p. The presence of uniformly distributed hard SiC_p in large amounts in the matrix of RDC alloy results in improved wear resistance. RDC composites with high volume of SiC_p have reported to have the non-dendritic grains that are less prone to wear which in turn lowered the volume of wear debris. Thus the decrease in wear rate of the metal matrix samples correlates well with the percentage of SiC_p with decreasing grain size.

4. Conclusions

1. In-house designed and fabricated Rheo-Die-Casting (RDC) equipment was successfully used for development both unreinforced and reinforced SiC_p particulate RDC Al-7.5 wt % Si-0.3 wt % Mg alloys under semisolid conditions.
2. RDC alloys as well as composites with improved both non-dendritic microstructure and uniform distributions of SiC_p particulates were produced.
3. Compared to HPDC alloy, RDC alloys have much improved microstructures showing very fine α_{Al} grains of about 20 µm with uniform distribution of spherical shaped Si particles in the matrix achieved without modification treatment of RDC alloy. In case of RDC composites, the grain size of the matrix is markedly decreased with increasing percentage of SiC_p reinforcement. This is due to the formation of semisolid condition promoted by SiC_p followed by controlled mechanical deformation through RDC process.
4. In general, both RDC alloy and composites exhibit very good resistance to wear under abrasive wear test. In case of RDC composites, the wear resistance was found to be nearly three times higher than that of RDC alloy. However the wear resistance of the RDC sample is higher in comparison to HPDC sample.
5. The improved wear behavior of both RDC alloy and composites can be attributed due to the presence of (i) fine grained non-dendritic microstructure, (ii) spherical shaped Si particles, (iii) good wettability and (iv) uniform distribution of SiC_p with matrix.

5. References

1. Gupta M, Ling S. Microstructure and mechanical properties of hypo/hyper-eutectic Al-Si alloys synthesized using a neat-net shape forming technique. J Alloys Compd. 1999;287(1-2):284-94.
2. Haga T, Kapranos P. Simple rheocasting processes. J Mater Process Technol. 2002;130-131:594-8.
3. Falak P, Niroumand B. Rheocasting of an Al-Si alloy. Scr Mater. 2005;53(1):53-7.
4. Fan Z, Fang X, Ji S. Microstructure and mechanical properties of rheo-diecast (RDC) aluminium alloys. Mater Sci Eng A. 2005;412(1-2):298-306. http://dx.doi.org/10.1016/j.msea.2005.09.001.
5. Wannasin J, Canyook R, Burapa R, Sikong L, Flemings MC. Evaluation of solid fraction in a rheocastaluminium die casting alloy by a rapid quenching method. Scr Mater. 2008;59(10):1091-4.
6. Salleh MS, Omar MZ, Syarif J, Mohammed MN. An overview of semisolid processing of aluminium alloys. ISRN. Mater Sci. 2013;2013:1-9.
7. Wu S, Zhong G, Wan L, an P, Mao Y. Microstructure and properties of rheo-diecast Al-20Si-2Cu-1Ni-0.4Mg alloy with direct ultrasonic vibration process. Trans Nonferrous Met Soc China. 2010;20:763-7.
8. Paes M, Zoqui EJ. Semi-solid behavior of new Al-Si-Mg alloys for thixoforming. Mater Sci Eng A. 2005;406(1-2):63-73.
9. Shabestari SG, Moemeni H. Effect of copper and solidification conditions on microstructure and mechanical properties of Al-Si-Mg alloys. J Mater Process Technol. 2004;153-154:193-8.
10. Guan RG, Zhao ZY, Li YD, Chen TJ, Xu SX, Qi PX. Microstructure and properties of squeeze cast A356 alloy processed with a vibrating slope. J Mater Process Technol. 2016;229:514-9.
11. Kolahdooz A, Dehkordi SA. Effect of important parameters in the production of Al-A356 alloy by semi-solid forming process. J. Mater. Proc. Res. Technol. 2018;333:1-10.
12. Sato T. Development of Deformation-Semisolid-Casting (D-SSC) process and applications to some aluminium alloys. J Mater Sci Technol. 2008;24:12-6.
13. Arrabal R, Mingo B, Pardo A, Mohedano M, Matykina E, Rodríguez I. Pitting corrosion of rheocast A 356 aluminium alloy in 3.5 wt % NaCl solution. Corros Sci. 2013;73:342-55. http://dx.doi.org/10.1016/j.corsci.2013.04.023.
14. Zheng Z, Ji Y, Mao W, Yue R, Liu Z. Influence of rheo-diecasting processing parameters on microstructure and mechanical properties of hypereutectic Al-30%Si alloy. Trans Nonferrous Met Soc China. 2017;27(6):1264-72. http://dx.doi.org/10.1016/S1003-6326(17)60147-X.
15. Hekmat-Ardakan A, Ajersch F. Effect of conventional and rheocasting processes on microstructural characteristics of hypereutectic Al–Si–Cu–Mg alloy with variable Mg content. J Mater Process Technol. 2010;210(5):767-75. http://dx.doi.org/10.1016/j.jmatprotec.2010.01.005.
16. Birol Y. Semi-solid processing of the primary aluminium die casting alloy A365. J Alloys Compd. 2009;473(1-2):133-8.
17. Tzamtzis S, Barekar NS, Hari Babu N, Patel J, Dhindaw D, Fan Z. Processing of advanced Al/SiC particulate metal matrix composites under intensive shearing: a novel Rheo-process. Compos, Part A Appl Sci Manuf. 2009;40(2):144-51.
18. Curle UA, Ivanchev L. Wear of semi-solid rheocastSiCp/Al metal matrix composites. Trans Nonferrous Met Soc China. 2010;20:852-6.
19. Gupta AK, Prasad BK, Pajnoo RK, Das S. Effect of T6 heat treatment on mechanical, abrasive and erosive-corrosive wear properties of eutectic Al-Si alloy. Trans Nonferrous Met Soc China. 2012;22(5):1041-50.
20. Esmaily M, Mortazavi N, Svensson JE, Jarfors AEW, Wessen M, Arrabal R, et al. On the microstructure and corrosion behavior

of AZ91/SiC composites produced by rheocasting. Mater Chem Phys. 2016;180:29-37.
21. Amirkhanlou S, Niroumand B. Fabrication and characterization of Al356/SiCp semisolid composites by injecting SiCp containing composite powders. J. Mater. Proc. Technol. 2012;212(4):841-7.
22. Cong X-S, Shen P, Wang Y, Jiang Q. Wetting of polycrystalline SiC by molten Al and Al-Si alloys. Appl Surf Sci. 2014;317:140-6.
23. Elmadagli M, Perry T, Alpas AT. A parametric study of the relationship between microstructure and wear resistance of Al-Si alloys. Wear. 2007;262(1-2):79-92.
24. Rao RN, Das S. Effect of sliding distance on the wear and friction behavior of as cast heat-treated Al-SiCp composites. Mater Des. 2011;32(5):3051-8.
25. Kori SA, Chandrashekharaiah TM. Studies on the dry sliding wear behavior of hypoeutectic and eutectic Al-Si alloys. Wear. 2007;263(1-6):745-55.
26. Basavakumar KG, Mukunda PG, Chakraborty M. Influence of grain refinement and modification on dry sliding wear behavior of Al-7Si and Al-7Si-2.5Cu cast alloys. J Mater Process Technol. 2007;186(1-3):236-245.
27. Chandrashekharaiah TM, Kori SA. Effect of grain refinement and modification on the dry sliding wear behiour of eutectic Al-Si alloys. Tribol Int. 2009;42(1):59-65.
28. Desale GR, Gandhi BK, Jain SC. Particle size effects on the slurry erosion of aluminium alloy (AA 6063). Wear. 2009;266(11-12):1066-71.
29. Basavarajappa S, Chandramohan G, Mukund K, Ashwin M, Prabu M. Dry sliding wear behavior of Al 2219/ SiC_p - Gr hybrid metal matrix composites. J. Mater. Perform. 2006;15(6):668-74. http://dx.doi.org/10.1361/105994906X150803.
30. Guo X, Guo Q, Nie J, Liu Z, Li Z, Fan G, et al. Particle size effect on the interfacial properties of SiC particle-reinforced Al-Cu-Mg composites. Mater Sci Eng A. 2018;711:643-9.
31. Bansal S, Saini TS. Mechanical and wear properties of SiC/ Graphite reinforced A1359 alloy-based metal matrix composite. Def Sci J. 2015;65(4):330-8.